BMB
Reports

In-silico and *In-vitro* based studies of *Streptomyces peucetius* CYP107N3 for oleic acid epoxidation

*Saurabh Bhattarai, Narayan Prasad Niraula, Jae Kyung Sohng & Tae-Jin Oh**
Institute of Biomolecule Reconstruction (IBR), Department of Pharmaceutical Engineering, SunMoon University, Asan 336-708, Korea

Certain members of the cytochromes P450 superfamily metabolize polyunsaturated long-chain fatty acids to several classes of oxygenated metabolites. An approach based on *in silico* analysis predicted that *Streptomyces peucetius* CYP107N3 might be a fatty acid-metabolizing enzyme, showing high homology with epoxidase enzymes. Homology modeling and docking studies of CYP107N3 showed that oleic acid can fit directly into the active site pocket of the double bond of oleic acid within optimum distance of 4.6 Å from the Fe. In order to confirm the epoxidation activity proposed by *in silico* analysis, a gene coding CYP107N3 was expressed in *Escherichia coli*. The purified CYP107N3 was shown to catalyze C_9-C_{10} epoxidation of oleic acid *in vitro* to 9,10-epoxy stearic acid confirmed by ESI-MS, HPLC-MS and GC-MS spectral analysis. [BMB Reports 2012; 45(12): 736-741]

INTRODUCTION

The cytochrome P450 (CYP) superfamily represents a highly diversified set of heme-containing enzymes found in bacteria, fungi, animals and plants (1). These enzymes are a major class of biocatalysts related to the oxidative metabolism of many drugs. Most often, this is brought about by the CYP metabolisms increasing the solubility of compounds facilitating metabolic processes within the cell.

Fatty acid-oxidizing enzymes have been the subject of an increasing number of studies in all organisms, since the products of their reactions exhibit fundamental biological activities (2-4). For instance, CYP epoxygenases convert ω3-poly unsaturated fatty acids, such as eicosapentaenoic acid or docosahexaenoic acid to epoxy-derivatives (5) which are potent dilators of coronary arterioles (6-8) or the pulmonary artery (9), and inhibit platelet aggregation (10). It is also well known that CYPs play a prominent role in oxidative metabolism. CYP102A1 (*Bacillus megaterium* BM-3), a bacterial CYP that closely resembles eukaryotic microsomal CYPs is mainly a ω-hydroxylase for arachidonic acid and a highly specific epoxygenase for eicosapentaenoic acid. Replacement of phenylalanine 87 (F87) with valine (V) converts CYP102A1 into a highly specific arachidonic acid epoxygenase (11). The epoxidation of polyunsaturated fatty acid double bonds, particularly of arachidonic acid, has generated much interest because of the biological activities of the resulting metabolites (12, 13). These epoxidation reactions of arachidonic acid ($C_{20:4}$) are catalyzed by members of the CYP2C subfamily and by the CYP2J2 isoform (14, 15). Human CYP4F8 and CYP4F12 isoforms are able to epoxidize docosahexaenoic acid ($C_{22:6}$) (16).

With an objective of finding a new epoxygenase from *Streptomyces* species, we carried out *in silico* analysis of all 23 CYPs present in the *Streptomyces* peuceitus. A BLAST search revealed CYP107N3 has high sequence identity with well characterized epoxygenases including OleP (*S. antibioticus*) and ChmPII (*S. bikiniensis*) (17, 18). Homology modeling and docking studies revealed oleic acid to be the best candidate for *in vitro* studies. Herein, we report the heterologous expression and functional characterization of *S. peucetius* CYP107N3 as oleic acid epoxidase which was screened for its putative epoxidase activity by *in silico* analysis.

RESULTS

Sequence alignment and homology modeling

The putative *S. peucetius* CYP107N3 gene encodes for 414 amino acids with a predicted molecular mass of 46 kDa. The overall G + C content of the gene is 71%, which is characteristic of such genes. The amino acid sequence of CYP107N3 was aligned with other epoxygenases by Clustal X. They showed 51% identity with OleP (*S. antibioticus*) and 48% identity with a ChmPII (*S. bikiniensis*) (data not shown). Based upon a PDB-BLAST search using ExPASy (2010) server, three highly homologous proteins CYP158A2 (PDB ID: 2D0E, 42% identity), CYP105A1 (PDB ID: 2ZBX, 40% identity) and CYP105P1 (PDB ID: 3E5L, 40% identity) were selected as templates to build a homology model of CYP107N3. Sequence alignment between CYP107N3 and other CYPs was performed using Align3D, followed by manual modification (Fig. 1A), and models were generated by MODELER (19). The final align-

*Corresponding author. Tel: +82-41-530-2677; Fax: +82-41-530-2279; E-mail: tjoh3782@sunmoon.ac.kr
http://dx.doi.org/10.5483/BMBRep.2012.45.12.080

Received 16 April 2012, Revised 23 May 2012, Accepted 6 July 2012

Keywords: Cytochrome P450, Epoxidation, Homology Modeling/docking; *In silico*, *Streptomyces peucetius*

ISSN: 1976-6696 (print edition) / 1976-670X (electronic edition)

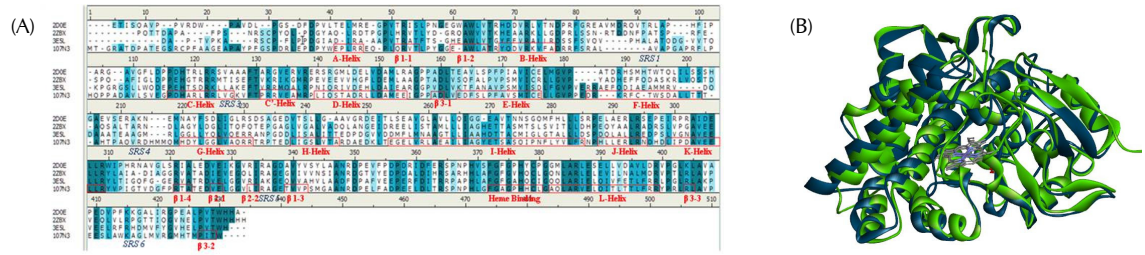

Fig. 1. (A) Multiple sequence alignment of CYP107N3 with three highly homologous templates CYP158A2 (PDB ID: 2D0E, 42% identity), CYP105A1 (PDB ID: 2ZBX, 40% identity) and CYP105P1 (PDB ID: 3E5L, 40% identity). Deep green color shows conserved residues in all three templates sequence, and red boxes indicate helixes or beta-sheets. (B) Superimposition of CYP107N3 model (blue) over CYP158A2 (green).

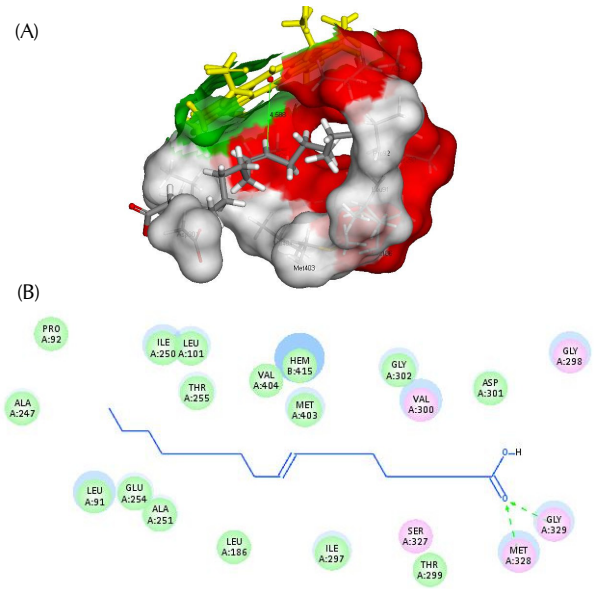

Fig. 2. (A) Oleic Acid docking into CYP107N3 model. The distance between iron in the porphyrin and C9 atom of oleic acid is 4.6 Å as shown by the green line. (B) 2D display of amino acids within active site surrounding the ligand. B:415 denotes the heme ligand. Amino acids with green circles represent residues involving in van der Waals interactions with the ligand, whereas those with pink circles interact with the ligand via a charge or polar based interaction. Two hydrogen bonds between carboxyl oxygen of the ligand and Met328/Gly329 are shown in green dashed lines.

ment was carefully evaluated and was found to match the conserved residues fairly well; thereafter, the model was superimposed over its highest homologue template CYP158A2 (Fig. 1B; CYP107N3 in blue and CYP158A2 in green). The RMSD of Cα, and backbone for the model and the template crystal structure, was found to be 1.107 Å and 1.083 Å, respectively. The model was also validated using the ProSa2003 z-score. The required negative scores, obtained for all the residues, further confirmed that the model was reliable (data not shown). The Ramachandran plot φ/ψ distribution of backbone conformation angles for each residue of the refined structure revealed that, 92.8% were in the favored region, 4.2% of amino acids were in allowed region, and 3.0% were in outlier region. These validation results consistently demonstrated that the CYP107N3 model was reasonable and could be employed for the further docking study. The model substrate oleic acid was docked into the CYP107N3 model using LigandFit (20), and the top binding mode for each, as adjudged by LigScore, was overlaid and displayed in the binding site (Fig. 2A). The distance between the unsaturated bond of oleic acid and the heme was 4.6 Å which is within the range for successful hydroxylation reaction to occur. The oleic acid chain was bound almost entirely via hydrophobic interactions with amino acid side chains (Pro92, Leu91, Leu101, Leu186, Ala247, Ala251, Gly302, Ile250, Ile297, Val404, Glu254, Thr255, Thr299, Met403 and Asp301) and via polar interactions (Gly298, Val300 and Ser327). Two hydrogen bonds, between carboxyl oxygen of oleic acid and Met328/Gly329, were also observed, further helping the stabilization of the ligand within the active site (Fig. 2B).

Expression and spectral analysis of CYP107N3

The expressed His-tag fused CYP107N3 was purified using Co^{2+} affinity chromatography where the target protein was eluted at 500 mM imidazole. The predicted molecular weight of the protein (46 kD) was subsequently confirmed by 12% SDS-PAGE (Fig. 3A). When substrate is unbound to a cytochrome, heme iron is in ferric form coordinated by six water molecules. In this state, heme iron shows absorbance at 420 nm. Substrate bound CYP, on the other hand, a hexa-coordinated heme iron is changed to a penta-coordinated state from perturbation of the electronic shell. This change in the water coordination causes a spin state shift of the Soret band from approximately 418 nm (representing the low-spin substrate free form), to around 390 nm for the high-spin, which results in a classical type I spectrum (21). Incubation of CYP107N3 with oleic acid results in a type I spectrum indicating oleic

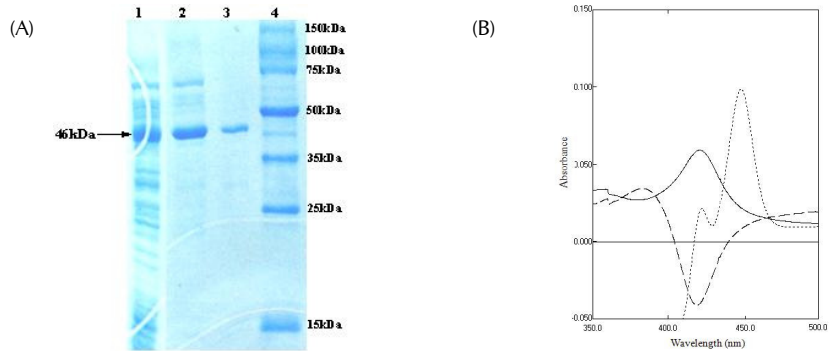

Fig. 3. (A) SDS-PAGE analysis of pN 107N3 expressed in *E. coli* BL21 (DE3). Lane 1, soluble fraction of cell lysate; lane 2, purified CYP107N3; lane 3, dialyzed fraction of purified CYP107N3; and lane 4, molecular marker. (B) Absorption spectra of CYP 107N3 in oxidized state as isolated (solid line), incubated with 1 μM of oleic acid showing Type I spectra (dashed line) and reduced CO-difference spectra (dotted line).

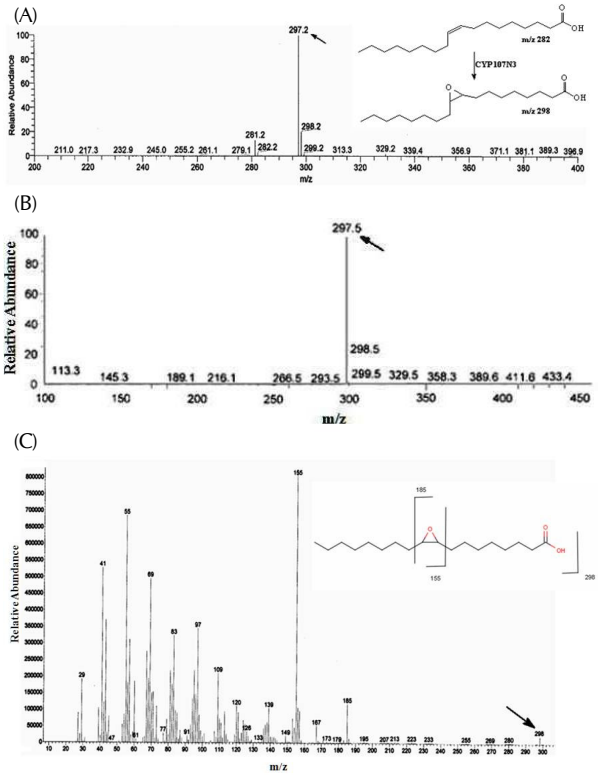

Fig. 4. (A) ESI-MS analysis of epoxide product 9,10-epoxystearic acid in negative mode. (B) LC-MS analysis of products from pNAJ128 recombinant strain of *E. coli* BL21(DE3) showing molecular ion $[M\text{-}H]^+$ at m/z = 297.5. (C) GC-MS analysis with fragmentation pattern for 9,10-epoxystearic acid isolated from *in vitro* reaction sample ([M] m/z = 298).

acid as a potential substrate. The CO binding spectra of CYP107N3 was determined as described in Materials and Method. CYP107N3 showed a characteristic absorbance at 450 nm for the $Fe^{II}(CO)$ complex, evident of an active form (Fig. 3B). The expression yield of CYP107N3 determined from the CO-difference spectra was 1,170 nmol l^{-1}.

Protein assay for epoxidation

The epoxidase activity of CYP107N3 was determined with oleic acid as a substrate. The protein extracts from *E. coli* mutant, harboring only expression vector (pET28a), were used as a negative control. The extracted product from the reaction sample was analyzed by ESI-MS showed a mass of 297.2, which is a possible epoxidated product (Fig. 4A). Subsequent LC/MS analysis of the peak clearly indicated an epoxidated product with a mass of 297.5 in negative mode (Fig. 4B). Furthermore, GC-MS analysis showed the major peak with *m/z* of 155 and 185 along with 298 which is characteristic mass fragmentation patterns of epoxidated oleic acid (Fig. 4C).

DISCUSSION

As epoxidated and hydroxylated fatty acids have gain grounds as valuable pharamaceutical and antimicrobial agents, the search for new fatty acid hydroxylase compounds, or novel engineering of current ones, has intensified. The hydroxylated fatty acid 7S,10S-dihydroxy-8E octadecanoic acid, isolated from *Pseudomonas aeruginosa*, has been found to stop the growth of the pathogenic yeast *Candida albicans*, whereas 7S,10S,12R-trihydroxy-8E-octadecenoic acid, isolated from same species, exhibits antimicrobial activity and curtails the rice blast fungus (*Magnaporthe grisea*) (22). *Candida* yeasts have been widely used for fatty acid oxygenation e.g. the production of α,ω-dicarboxylic acids. Apart from yeast, several bacteria such as *Pseudomonades*, *Bacilli* or *Rhodococci* are able to hydroxylate fatty acid in a terminal or subterminal manner (23, 24). For enzymatic synthesis of hydroxyl fatty acid, *E. coli* transformed with a P450BM-3 has been used with a fatty acid uptake system (25, 26) but still biocatalytic hydroxylation and epoxidation of fatty acids by bacterial CYP is in its infancy. Moreover, plant and animal CYP has been studied and found to be better oleic acid epoxidase. *Arabidopsis thaliana* CYP77A4 was the first CYP which was determined to be able to catalyse the epoxidation of free fatty acid in plants (27). Similarly, P4502CAA and P4502C2, from the rabbit, have also been studied for the epoxidation of oleic acid (28). To find a new epoxidase from *Streptomyces sp.*, we conducted a BLAST

search and identified CYP107N3 as having high identity with previously reported epoxidase from *Streptomyces sp*. Homology modeling and docking studies of CYP107N3 revealed oleic acid to be the best candidate for *in vitro* studies. Previously, the crystal structure of CYP102A1 in complex with palmitoleic acid has shown that the acid group binds to positively charged or hydrogen-bonding residues near the entrance of the hydrophobic substrate access channel, while the alkyl chain penetrates the channel, and reaches the catalytic center in a geometric arrangement allowing hydroxylation to occur (29), consistent with the docking of oleic acid determined in this study. The carboxyl groups form hydrogen-bonds with Met328 and Gly329 residues near the entrance. The distance of 4.6 Å from heme iron to the site of epoxidation was the optimum distance for reaction to occur. To establish oleic acid as a substrate of CYP107N3, the CYP was expressed in *E. coli*. The substrate binding assay conducted with oleic acid showed a Type I spectrum, indicating that oleic acid binds at the catalytic site of CYP107N3 near the heme. The reaction product obtained from *in vitro* enzyme assay, using spinach ferredoxin and ferredoxin reductase as redox partner, was analyzed and found to be the epoxidated product of oleic acid, i.e. 9,10-epoxystearic acid. Further studies investigating whether CYP107N3 can also accept other substrates are ongoing, for the introduction of epoxy substituent into different fatty acid derivatives.

MATERIALS AND METHODS

Bacterial strains, plasmids and growth conditions

Standard methods were used for DNA cloning, plasmid isolation, and restriction enzyme digestion (30, 31). *E. coli* strains were grown at 37°C in Luria Bertani (LB) media in both liquid and agar plates supplemented with the appropriate amount of antibiotic (ampicillin 100 μg ml^{-1}). pGEM-T easy vector (Promega, USA) and pET-28a(+) (Novagen, Germany) were used for the cloning of polymerase chain reaction (PCR) products and for the expression of the gene, respectively. *E. coli* XL1-Blue (MRF) (Stratagene, USA) was used as a host cell for the preparation of recombinant plasmid and manipulation of DNA, whereas *E. coli* BL21 (DE3) (Stratagene, USA) was used as the host for the expression. Reagent grade chemicals were purchased from Sigma/Aldrich or Merck, UK. In some cloning experiments, 0.4 mM isopropyl-β-thiogalactopyranoside (IPTG) and 50 mM 5-bromo-4-chloro-3-indolyl-β-D-galactopyranoside (X-gal) were included in the LB agar plates for screening.

Sequence analysis and homology modeling

The computer-based analyses and comparison of protein sequences were performed using the programs BLAST, FASTA, CLUSTALW and GENEDOC. The homology modeling of CYP107N3 and docking were performed using Accelrys Discovery Studio V3.1 (Accelrys Software Inc., San Diego, CA, USA). The homologue search was done from the ExPASy web site (http://swissmodel.expasy.org). The structures of three highly homologous proteins, 2D0E (CYP158A2, 2.15 Å, length 407 aa) (32), 2ZBX (CYP105A1, 1.5 Å, length 412 aa) (33) and 3E5L (CYP105P1, 2.40 Å, length 403 aa) (34) were selected as templates for modeling. The final 3D model was generated by MODELER, an original program (19) that performed automatic protein homology modeling and loop modeling for CYP107N3. The refined model was validated with ProSa2003 (35), and Ramachandran Plot (36). RSMD (Root Mean Square Deviation) analysis of the predicted model from its templates was calculated using SUPERPOSE (37). Substrate for docking was drawn using a sketch toolbar application and converted to stereo-chemically correct configuration and optimized by Dreiding-like force-field in DS V3.1. The protein-ligand interaction study was performed using LigandFit/LigandScore (20), an automated tool for protein-small molecule docking/scoring.

Construction of recombinant plasmid

Recombinant pN107N3 was constructed for *E. coli* hosts as following. A set of primers 107N3F (5′-GTC GAA TTC ATG ACG GGC CGG GCG ACC GA-3′) and 107N3R (5′-AGT AAG CTT TCA CCA GGT GAT CGG CAT GG-3′) (the underlined letters indicate the restriction sites) was used for the amplification of CYP107N3 coding region (GenBank accession no. CAE53712). Polymerase chain reaction (PCR) was performed in a thermocycler (Takara, Japan). The amplification conditions for PCR were: 94°C for 7 min, followed by 30 cycles of 94°C for 1 min, 60°C for 1 min, 72°C for 1 min and finally 72°C for 10 min. DNA amplification was performed in a total volume of 20 μl containing 5 μl PCR Mix (Genotech Co., Korea). The PCR products (1,245 bp) were cloned into pGEM-T (Promega, USA) and sequenced prior to cloning into the expression vector in order to verify that no mutation had been introduced during PCR amplification. The purified PCR product was again cloned into the *Eco*RI-*Hin*dIII sites of the pET-28a(+) vector. The recombinant expression vector pN107N3 was introduced into *E. coli* BL21 (DE3) by heat-pulse transformation (31).

Expression and purification of His-tag fused protein

E. coli BL21 (DE3) was transformed with the recombinant plasmid (pN107N3), and the overnight culture was diluted 1 : 50 in fresh medium. IPTG was added to a final concentration of 0.4 mM when the culture reached an optical density at 600 nm (OD_{600}) of 0.7, and the induction was carried out for 20 h in a 20°C shaker. 1 mM 5-aminolevulinic acid (ALA) and 0.5 mM FeCl3 were added to the culture medium 10 min before IPTG induction in order to increase the yield of active CYP (38). After harvest, the cells were washed with 25 ml of 50 mM phosphate buffer (pH 7.5) and resuspended in 2 ml of storage buffer [10% glycerol along with 1 mM DTT, 1 mM PMSF and 0.1 mM EDTA in 50 mM potassium phosphate buffer (pH 7.6)]. The cell pellets were disrupted by ultrasonication, and the crude cell extract was obtained by centrifugation at 12,000xg for 20 min. The molecular masses of the denatured proteins were observed in SDS-PAGE analyses

compared with standard molecular mass protein markers (Novagen, USA). His-tag fused protein in crude cell extracts was purified by immobilized Co^{2+}-affinity chromatography (TALON, USA) according to the manufacturer's instructions. The proteins were eluted with a linear gradient of imidazole (from 10 to 500 mM) in water. The pure fractions were dialyzed with storage buffer (50 mM phosphate buffer, pH 7.5) and the purified proteins were analyzed by 12% SDS-PAGE.

Protein concentration and spin-state shift determination

The CYP content was determined as described previously (39). Briefly, 0.5 ml samples (crude or purified) were diluted in 4.5 ml of 50 mM potassium phosphate buffer (pH 7.6) with 1 mM EDTA and 10% (v/v) glycerol, and dithionite-reduced carbon monoxide difference spectra at 450 and 490 nm were measured. To perform this, a few crystals of sodium dithionite were added to the CYP-rich fraction obtained from the heterologously expressed strains, and were then mixed and divided into two cuvettes. The mixture was then saturated with 30 to 40 bubbles of CO at a rate of about 1 bubble per second. The absorbance difference between reduced CYP and CO bound CYP was measured using an extinction coefficient of the unreduced form ($\varepsilon = 91$ mM^{-1} cm^{-1}). To determine the spin-state shift upon substrate binding, 1 μM of protein in buffer (50 mM potassium phosphate buffer, pH 7.6) was incubated with 1 μM of substrate dissolved in ethanol in sample cuvette. The spectral changes between 350 and 500 nm was recorded. The reference cuvette contained the same concentration of protein and an equal volume of ethanol, but with no substrate.

Reconstituted assay of CYP107N3 with oleic acid

The activity of CYP107N3 was determined with oleic acid as a substrate. The reaction mixture consisted of 5 μM spinach ferredoxin, 0.1 unit of ferredoxin reductase, 4 μM CYP107N3, 1 mM NADH and 1 mM oleic acid, 10 mM of glucose 6-phosphate and 0.24 unit of glucose 6-phosphate dehydrogenase in 50 mM potassium buffer. The reaction mixtures were incubated at 37°C for 6 h, and an equal quantity of ethyl acetate was added to stop the reaction at the end of the incubation, which was followed by centrifugation to obtain the supernatant. The extract was analyzed by electron spray ionization-mass spectrometry (ESI-MS), high performance liquid chromatography-mass spectrometry (HPLC-MS) and gas chromatography-mass spectrometry (GC-MS) to determine product formation. The ESI-MS analysis was carried out with a probe temperature of 392°C and a source voltage of 31.2 V using Finnigan AQA (UK) mass spectrophotometer. Samples were injected via a 10-μl loop and were transferred at a flow rate of 1 ml min^{-1} using methanol as a solvent. The HPLC-MS for epoxidation of oleic acid was performed under the following conditions: column, Mightysil RP-18 GP (150 × 4.6 mm I.D., Kanto Chemical, Tokyo); gradient solvent system, water/methanol/acetonitrile (52/8/40; v/v/v). Analysis of the product was carried out by GC-MS (Agilent 59731) inert MSD, equipped with HP-5ms column. The conditions for GC-MS analysis was as follows, the injector and detector temperatures were set at 250°C and 285°C, respectively, with helium as carrier gas. Sample (1 μl) was injected for analysis. The column temperature was maintained at 180°C for 2 min, increased to 300°C at a rate of 8°C min^{-1}, and held at 300°C for 5 min. Conversion products were identified by their characteristic mass fragmentation patterns.

Acknowledgements

This research was supported by Basic Science Research Program through the National Research Foundation of Korea (NRF) funded by Ministry of Education, Science and Technology (2011-0003461, 2011-0026856).

REFERENCES

1. Werck-Reichhart, D. and Feyereisen, R. (2000) Cytochromes P450: a success story. *Genome Biol*. **1**, 3003.1-3003.9.
2. Funk, C. D. (2001) Prostaglandins and leukotrienes: advances in eicosanoid biology. *Science* **294**, 1871-1875.
3. Blee, E. (2002) Impact of phyto-oxylipins in plant defense. *Trends Plant Sci*. **7**, 315-322.
4. Noverr, M. C., Erb-Downward, J. R. and Huffnagle, G. B. (2003) Production of eicosanoids and other oxylipins by pathogenic eukaryotic microbes. *Clin. Microbiol. Rev*. **16**, 517-533.
5. Fer, M., Goulitquer, S., Dreano, Y., Berthou, F., Corcos, L. and Amet, Y. (2006) Determination of polyunsaturated fatty acid monoepoxides by high performance liquid chromatography-mass spectrometry. *J. Chromatogr. A* **1115**, 1-7.
6. Lauterbach, B., Barbosa-Sicard, E., Wang, M. H., Honeck, H., Kargel, E., Theuer, J., Schwartzman, M. L., Haller, H., Luft, F. C., Gollasch, M. and Schunck, W. H. (2002) Cytochrome P450-dependent eicosapentaenoic acid metabolites are novel BK channel activators. *Hypertension* **39**, 609-613.
7. Ye, D., Zhang, D., Oltman, C., Dellsperger, K., Lee, H. C. and VanRollins, M. (2002) Cytochrome p-450 epoxygenase metabolites of docosahexaenoate potently dilate coronary arterioles by activating large-conductance calcium-activated potassium channels. *J. Pharmacol. Exp. Ther*. **303**, 768-776.
8. Hercule, H. C., Salanova, B., Essin, K., Honeck, H., Falck, J. R., Sausbier, M., Ruth, P., Schunck, W. H., Luft, F. C. and Gollasch, M. (2007) The vasodilator 17,18-epoxyeicosatetraenoic acid targets the pore-forming BK alpha channel subunit in rodents. *Exp. Physiol*. **92**, 1067-1076.
9. Morin, C., Sirois, M., Echave, V., Rizcallah, E. and Rousseau, E. (2009) Relaxing effects of 17(18)-EpETE on arterial and airway smooth muscles in human lung. *Am. J. Physiol. Lung Cell Mol. Physiol*. **296**, L130-L139.
10. Van Rollins, M. (1995) Epoxygenase metabolites of docosahexaenoic and eicosapentaenoic acids inhibit platelet aggregation at concentrations below those affecting thromboxane synthesis. *J. Pharmacol. Exp. Ther*. **274**, 798-804.
11. Graham-Lorence, S., Truan, G., Peterson, J. A., Falck, J. R., Wei, S., Helvig, C. and Capdevila, J. H. (1997) An active site

substitution, F87V, converts cytochrome P450 BM-3 into a regio- and stereoselective (14S,15R)-arachidonic acid epoxygenase. *J. Biol. Chem.* **272**, 1127-1135.
12. Roman, R. J. (2002) P-450 metabolites of arachidonic acid in the control of cardiovascular function. *Physiol. Rev.* **82**, 131-185.
13. Fleming, I. (2007) Epoxyeicosatrienoic acids, cell signaling and angiogenesis. *Prostaglandins Other Lipid Mediat.* **82**, 60-67.
14. Zeldin, D. C., Moomaw, C. R., Jesse, N., Tomer, K. B., Beetham, J., Hammock, B. D. and Wu, S. (1996) Biochemical characterization of the human liver cytochrome P450 arachidonic acid epoxygenase pathway. *Arch. Biochem. Biophys.* **330**, 87-96.
15. King, L. M., Ma, J., Srettabunjong, S., Graves, J., Bradbury, J. A., Li, L., Spiecker, M., Liao, J. K., Mohrenweiser, H. and Zeldin, D. C. (2002) Cloning of CYP2J2 gene and identification of polymorphisms. *Mol. Pharmacol.* **61**, 840-852.
16. Stark, K., Wongsud, B., Burman, R. and Oliw, E. H. (2005) Oxygenation of polyunsaturated long chain fatty acids by recombinant CYP4F8 and CYP4F12 and catalytic importance of Tyr-125 and Gly-328 of CYP4F8. *Arch. Biochem. Biophys.* **441**, 174-181.
17. Shah, S., Xue, Q., Tang, L., Carney, J. R., Betlach, M. and McDaniel, R. (2000) Cloning, characterization and heterologous expression of polyketide synthase and P-450 oxidase involved in the biosynthesis of the antibiotic oleandomycin. *J. Antibiot.* **53**, 502-508.
18. Ward, S. L., Hu, Z., Schirmer, A., Reid, R., Revill, W. P., Reeves, C. D., Petrakovsky, O. V., Dong, S. D. and Katz, L. (2004) Chalcomycin biosynthesis gene cluster from *Streptomyces bikiniensis*: novel features of an unusual ketolide produced through expression of the chm polyketide synthase in *Streptomyces fradiae*. *Antimicrob. Agent Chemother.* **48**, 4703-4712.
19. Sali, A., Pottertone, L., Yuan, F., Van Vlijmen, H. and Karplus, M. (1995) Evaluation of comparative protein modeling by MODELLER. *Proteins* **23**, 318-326.
20. Venkatachalam, C. M., Jiang, X., Oldfield, T. and Waldman, M. (2003) LigandFit: a novel method for the shape-directed rapid docking of ligands to protein active sites. *J. Mol. Graph. Model* **21**, 289-307.
21. Schenkman, J. B., Sligar, S. G. and Cinti, D. L. (1981) Substrate interaction with cytochrome P-450. *Pharmacol. Ther.* **12**, 43-71.
22. Kuo, T. M. and Lanser, A. C. (2003) Factors influencing the production of novel compound, 7,10-dihydroxy-8(e)- octadecanoic acid, by *pseudomonas aeruginosa* PR3 (NRRL B-18602) in batch cultures. *Curr. Microbiol.* **47**, 186-197.
23. Kuo, T. M., Lanser, A. C., Nakamura, L. K. and Hou, C. T. (2000) Production of 10-ketostearic acid and 10-hydroxystearic acid by strains of *Sphingobacterium thalophilum* isolated from composted manure. *Curr. Microbiol.* **40**, 105-109.
24. Kuo, T. M., Nakamura, L. K. and Lanser, A. C. (2002) Conversion of fatty acid by Bacillus sphaericus-like organisms. *Curr. Microbiol.* **45**, 265-271.
25. Schneider, S., Wubbolts, M. G., Sanglard, D. and Witholt, B. (1998) Biocatalyst engineering by assembly of fatty acid transport and oxidation activities for in vivo application of cytochrome P450BM-3 monooxygenase. *Appl. Environ. Microbiol.* **64**, 3784-3790.
26. Schneider, S., Wubbolts, M. G., Oesterhelt, G., Samglard, D. and Witholt, B. (1999) Controlled regioselectivity of fatty acid oxidation by whole cells producing cytochrome P450BM-3 monooxygenase under varied dissolved oxygen concentration. *Biotechnol. Bioeng.* **64**, 333-341.
27. Sauveplane, V., Kandel, S., Kastner, P. E., Ehlting, J., Compagnon, V., Werck-Reichhart, D. and Pinot, F. (2009) *Arabidopsis thaliana* CYP77A4 is the first cytochrome P450 able to catalyze the epoxidation of free fatty acids in plants. *FEBS J.* **276**, 719-735.
28. Laethem, R. M., Balazy, M. and Koop, D. R. (1996) Epoxidation of C18 unsaturated fatty acids by cytochromes P4502C2 and P4502CAA. *Drug Metab. Dispos.* **24**, 664-668.
29. Ortiz de Montellano, P. R., Chan, W. K., Tuck, S. F., Kaikaus, R. M., Bass, N. M. and Peterson, J. A. (1992) Mechanism-based probes of the topology and function of fatty acid hydroxylases. *FASEB J.* **6**, 695-699.
30. Kieser, T., Bibb, M. J., Buttner, M. J., Chater, K. F. and Hopwood, D. A. (2000) Practical *Streptomyces* Genetics. 2nd ed. The John Innes Centre Foundation, Norwich, UK.
31. Sambrook, J. and Russell, D. W. (2001) Molecular cloning, a laboratory manual. 3rd ed. Cold Spring Harbor Laboratory, Cold Spring Harbor, NY.
32. Sugimoto, H., Shinkyo, R., Hayashi, K., Yoneda, S., Yamada, M., Kamakura, M., Ikushiro, S., Shiro, Y. and Sakaki, T. (2008) Crystal structure of CYP105A1 (P450SU-1) in complex with 1 alpha,25-dihydroxyvitamin D3. *Biochemistry* **47**, 4017-4027.
33. Zhao, B., Guengerich, F. P., Voehler, M. and Waterman, M. R. (2005) Role of active site water molecules and substrate hydroxyl groups in oxygen activation by cytochrome P450 158A2: A new mechanism of proton transfer. *J. Biol. Chem.* **280**, 42188-42197.
34. Xu, L. H., Fushinobu, S., Ikeda, H., Wakagi, T. and Shoun, H. (2009) Crystal structure of cytochrome P450 105P1 from *Streptomyces avermitilis*: conformational flexibility and histidine ligation state. *J. Bacteriol.* **191**, 1211-1219.
35. Sippl, M. J. (1993) Recognition of errors in three-dimensional structures of proteins. *Proteins* **17**, 355-362.
36. Lovell, S. C., Davis, I. Q., Arendall III, W. B., de Bakker, P. I., Word, J. M., Prisant, M. G., Richardson, J. S. and Richardson, D. C. (2003) Structure validation by Calpha geometry: phi, psi and Cbeta deviation. *Proteins* **50**, 437- 450.
37. Maiti, R., Van Domselaar, G. H., Zhang, H. and Wishart, D. S. (2004) SuperPose: a simple server for sophisticated structural superposition. *Nucleic Acids Res.* **32**, W590- W594.
38. Hussain, H. A. and Ward, J. M. (2003) Enhanced heterologous expression of two *Streptomyces* griseolus cytochrome P450s and *Streptomyces coelicolor* ferredoxin reductase as potentially efficient hydroxylation catalysts. *Appl. Environ. Microbiol.* **69**, 373-382.
39. Omura, T. and Sato, R. (1964) The carbon monoxide- binding pigment of liver microsomes. I. Evidence for its hemoprotein nature. *J. Biol. Chem.* **239**, 2370-2378.